

# MTPano: Multi-Task Panoramic Scene Understanding via Label-Free Integration of Dense Prediction Priors

JINGDONG ZHANG, Texas A&M University, USA  
 XIAOHANG ZHAN, Adobe, USA  
 LINGZHI ZHANG, Adobe, USA  
 YIZHOU WANG, Adobe, USA  
 ZHENGMING YU, Texas A&M University, USA  
 JIONGHAO WANG, Texas A&M University, USA  
 WENPING WANG, Texas A&M University, USA  
 XIN LI, Texas A&M University, USA

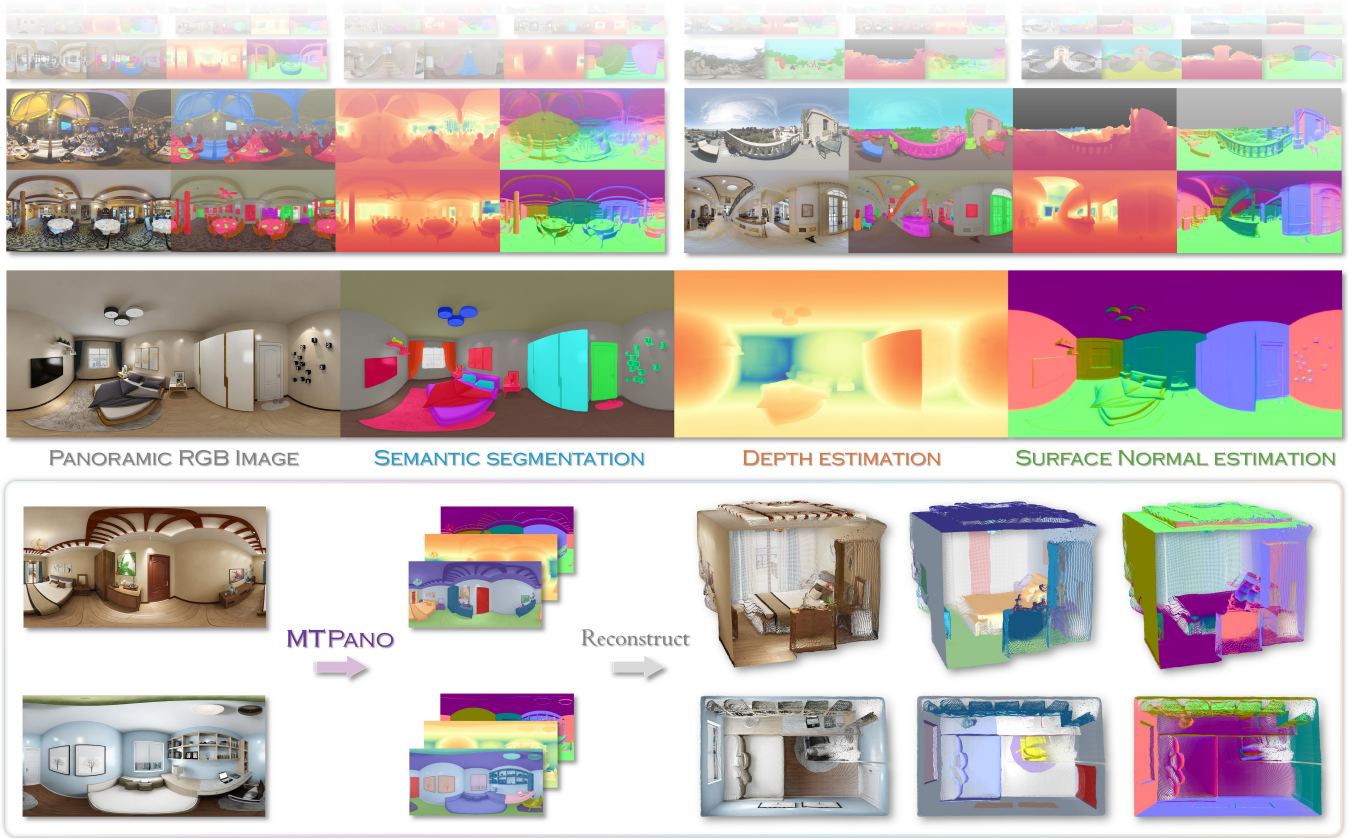


Fig. 1. **Panoramic Scene Understanding via MTPano.** We introduce MTPano, a multi-task foundation model for panoramic dense scene parsing.

Comprehensive panoramic scene understanding is critical for immersive applications, yet it remains challenging due to the scarcity of high-resolution, multi-task annotations. While perspective foundation models have achieved

success through data scaling, directly adapting them to the panoramic domain often fails due to severe geometric distortions and coordinate system discrepancies. Furthermore, the underlying relations between diverse dense prediction tasks in spherical spaces are underexplored. To address these challenges, we propose MTPano, a robust multi-task panoramic foundation model established by a label-free training pipeline. First, to circumvent data scarcity, we leverage powerful perspective dense priors. We project panoramic images into perspective patches to generate accurate, domain-gap-free pseudo-labels using off-the-shelf foundation models, which are then

Authors' Contact Information: Jingdong Zhang, Texas A&M University, College Station, Texas, USA, jdzhang@tamu.edu; Xiaohang Zhan, Adobe, USA, xiaohangzhan@outlook.com; Lingzhi Zhang, Adobe, USA, lingzzha@adobe.com; Yizhou Wang, Adobe, USA, wyzjack990122@gmail.com; Zhengming Yu, Texas A&M University, College Station, Texas, USA, yuzhengming@tamu.edu; Jionghao Wang, Texas A&M University, College Station, Texas, USA, jionghao@tamu.edu; Wenping Wang, Texas A&M University, College Station, Texas, USA, wenping@tamu.edu; Xin Li, Texas A&M University, College Station, Texas, USA, xinli@tamu.edu.

re-projected to serve as patch-wise supervision. Second, to tackle the interference between task types, we categorize tasks into rotation-invariant (e.g., depth, segmentation) and rotation-variant (e.g., surface normals) groups. We introduce the Panoramic Dual BridgeNet (PD-BridgeNet), which disentangles these feature streams via geometry-aware modulation layers that inject absolute position and ray direction priors. To handle the distortion from equirectangular projections (ERP), we incorporate ERP token mixers followed by a dual-branch BridgeNet for interactions with gradient truncation, facilitating beneficial cross-task information sharing while blocking conflicting gradients from incompatible task attributes. Additionally, we introduce auxiliary tasks (image gradient, edge distance field, point map estimation) to fertilize the cross-task learning process. Extensive experiments demonstrate that MTPano achieves state-of-the-art performance on multiple benchmarks and delivers competitive results against task-specific panoramic specialist foundation models.

CCS Concepts: • **Computing methodologies** → **Scene understanding**; **Multi-task learning**; *Image segmentation*; *Reconstruction*.

Additional Key Words and Phrases: Panoramic Image Understanding, Foundation Models, 360-Degree Vision

## 1 Introduction

Panoramic scene understanding has become a cornerstone of immersive technologies, empowering applications ranging from Virtual Reality (VR) content creation to ego-centric robot navigation. Unlike narrow field-of-view (FoV) perspective images, 360° panoramic images offer a holistic observation of the surroundings, necessitating a comprehensive interpretation of geometry (e.g., depth, surface normals) and semantics. Recent years have witnessed remarkable progress in dense prediction tasks [Cai et al. 2023; Laina et al. 2016; Ranftl et al. 2021; Vandenhende et al. 2020; Yang et al. 2020; Ye and Xu 2022], where foundation models [Kirillov et al. 2023; Lin et al. 2025; Yang et al. 2024a,b; Zhang et al. 2025d] have demonstrated exceptional capabilities in parsing complex perspective scenes. This success has naturally catalyzed a surging interest in exploring foundational perception models in the panoramic domain.

Inspired by the progress in the perspective domain, panoramic dense prediction is also witnessing a thriving era, with emerging research striving for high-fidelity spherical scene understanding [Cao et al. 2025; Huang et al. 2024a; Li et al. 2025; Lin et al. 2025; Zheng et al. 2024]. However, a major impediment remains: the development of these systems is typically data-driven, yet obtaining high-quality, manually collected pixel-wise annotations for 360° images is prohibitively expensive and labor-intensive, especially when extended to multiple tasks. To mitigate this data dependency, recent specialists have sought to harness abundant perspective resources. For instance, DA<sup>2</sup> [Li et al. 2025] synthesizes panoramic training data via perspective-to-sphere projection, while PanDA [Cao et al. 2025] distills priors from perspective foundation models [Yang et al. 2024a] using semi-supervised adaptation. Despite their success, these approaches operate in isolation, treating each modality as a standalone problem. This fragmentation overlooks the critical synergy between tasks (where semantic boundaries can spatially constrain depth discontinuities and vice versa [Vandenhende et al. 2020]). Furthermore, extending these single-task adaptation strategies to a multi-task setting requires more dedicated designs, as avoiding conflicts and

excavating mutual relevances among diverse attributes in a sphere is challenging.

Ideally, Multi-Task Learning (MTL) offers a unified solution to these issues. In the perspective domain, MTL frameworks [Vandenhende et al. 2020; Xu et al. 2018; Ye and Xu 2022; Zhang et al. 2025b] are well-established, primarily focusing on resolving task interference to maximize beneficial feature sharing. However, directly transferring these paradigms to the panoramic domain faces two distinct challenges. First, unlike single-task adaptation, jointly learning diverse dense predictions on a sphere induces severe conflicts. We observe that dense tasks benefit from different priors due to the different responses of coordinate transformations: rotation-invariant tasks (e.g., depth, semantic segmentation) depend solely on relative spatial context and should remain consistent when a transformation is applied, whereas rotation-variant tasks (e.g., surface normals) are strictly tied to the camera coordinates and are orientation-sensitive. Naively sharing features between these conflicting groups leads to *negative transfer*, where cross-task interference leads to mutual degradation. Second, standard perspective MTL architectures are ill-equipped to handle the non-uniform Equirectangular Projection (ERP) distortion. They lack specific mechanisms to model dependencies under ERP distortion while simultaneously decoupling the aforementioned conflicting task attributes. Consequently, simply applying perspective MTL methods to panoramas results in suboptimal performance.

To address these challenges, we introduce MTPano, a label-free framework that establishes a unified multi-task panoramic foundation model by taming dense perspective priors. Our approach tackles the aforementioned hurdles from both data and model perspectives. At the data level, we circumvent the need for manual annotation by integrating knowledge from multiple off-the-shelf perspective foundation models. We project the panoramic image into multiple perspective patches to obtain distortion-free pseudo-labels and then re-project them back as spherical patches for patch-wise supervision. This strategy allows us to leverage the vast knowledge of existing models while preventing overfitting to projection artifacts. At the model level, to resolve the conflict between tasks, we propose the Panorama-Dual-BridgeNet (PD-BridgeNet). Drawing inspiration from BridgeNet [Zhang et al. 2025b], we design a dual-branch architecture that explicitly disentangles rotation-invariant and rotation-variant feature streams. We employ a distortion-aware ERP Token Mixer to handle spherical distortions, and further disentangle the streams by injecting absolute position and ray direction priors into the variant branch via geometry-aware modulation layers. Crucially, we devise an asymmetric bridge mechanism with Truncated Gradient Flow: it allows beneficial information to flow between branches while blocking conflicting gradients, ensuring that invariant features are not corrupted by variant supervision and vice versa. Furthermore, we integrate dense auxiliary tasks (including Image Gradient, Edge Distance Field (EDF), and Metric Point Map) to introduce extra dense priors (e.g. rotation-invariant boundary and texture priors from Image Gradient, coordinate-related geometry priors from metric point maps), facilitating the cross-task learning process.

In summary, our contributions are three-fold:

- We propose MTPano, a multi-task panoramic understanding foundation model training under a label-free pipeline by effectively handling perspective dense priors from strong pretrained perspective specialist models.
- We identify the critical conflicts between rotation-invariant and -variant features in panoramic MTL and propose PD-BridgeNet, incorporating geometric feature modulation layers, distortion-aware token mixing, and a gradient-truncated bridge mechanism to harmonize conflicting features and improve cross-task consistency.
- Extensive experiments demonstrate that MTPano achieves state-of-the-art performance on multiple benchmarks, and also performs robustly on in-the-wild test cases.

## 2 Related Work

### 2.1 Foundational Understanding Models

The paradigm of computer vision has significantly shifted from training task-specific models on limited datasets to developing large-scale foundational models driven by massive data and scaling laws. Powered by the Vision Transformer (ViT) [Dosovitskiy et al. 2020] and self-supervised pretraining methods [He et al. 2022; Oquab et al. 2023; Siméoni et al. 2025], modern foundation models demonstrate exceptional generalization capabilities. In the realm of segmentation, Segment Anything (SAM) [Kirillov et al. 2023] utilizes a promptable mask decoder trained on the SA-1B dataset, establishing a new standard for zero-shot generalization. Following this, models like OpenScene [Peng et al. 2023] and DINO-X [Ren et al. 2024] have further extended open-vocabulary understanding to 3D and generic object detection. For geometry estimation, Depth Anything (v1/v2) [Yang et al. 2024a,b] demonstrates the power of data scaling for robust relative depth estimation. To resolve scale ambiguity and ensure geometric consistency, Metric3D [Hu et al. 2024; Yin et al. 2023] and MoGe [Wang et al. 2025b,c] introduce canonical camera transformations and coordinate-map representations to recover accurate metric depth and surface normals. Furthermore, Marigold [Ke et al. 2024] and Geowizard [Fu et al. 2024] repurpose latent diffusion models to leverage rich generative priors for state-of-the-art zero-shot generalization. These developments in specific domains suggest that leveraging such robust, general-purpose representations is a promising pathway to solve domain-specific challenges where labeled data is scarce.

### 2.2 Multi-Task Dense Prediction

Multi-Task Learning (MTL) for dense prediction [Cao et al. [n. d.]; Chavhan et al. 2025; Gao et al. 2019; Liu et al. 2019; Lu et al. 2024; Misra et al. 2016; Tang et al. 2025; Tian et al. 2024; Vandenhende et al. 2020; Xu et al. 2018; Yang et al. 2023, [n. d.]; Ye and Xu 2022, 2023a,b; Zhang et al. 2023a, 2025b, 2018, 2019] aims to learn a unified representation for pixel-wise tasks (e.g., semantic segmentation, depth estimation) to improve efficiency and performance. Early CNN-based approaches focused on decoder-focused feature fusion, such as Cross-Stitch Networks [Misra et al. 2016] and NDDR-CNN [Gao et al. 2019], which learn linear combinations of task features. To explicitly model task correlations, PAD-Net [Xu et al. 2018] introduced

a multi-modal distillation module to utilize intermediate predictions as priors, while MTI-Net [Vandenhende et al. 2020] proposed multi-scale task interactions to refine features at different resolutions. With the advent of Transformers, recent works have exploited global context for better task synergy. InvPT [Ye and Xu 2022] employs an inverted pyramid transformer to model global pixel and task interactions. TaskPrompter [Ye and Xu 2023b] and TaskExpert [Ye and Xu 2023a] introduce dynamic prompting and mixture-of-experts mechanisms to disentangle task-specific and task-generic information. More recently, BridgeNet [Zhang et al. 2025b] proposes to leverage bridge features as effective intermediate representations for cross-task interactions, 3D-aware MTL [Li et al. 2023; Wang et al. 2025a] extends the multi-task learning to 3D space and multi-view aspect. Beyond deterministic approaches, recent studies have also explored partially supervised MTL settings, such as DiffusionMTL [Ye and Xu 2024] and HiTTs [Zhang et al. 2025c]. However, most existing MTL architectures are tailored for perspective images. Directly applying them to panoramic domains fails to address the unique geometric conflicts and distortions inherent in spherical data.

### 2.3 Panoramic Understanding Models

Panoramic scene understanding is critical for providing a holistic view of the environment, but suffers from Equirectangular Projection (ERP) distortion and data scarcity. Some works addressed distortion by designing latitude-adaptive window partition [Shen et al. 2022] or utilizing specially designed embeddings like spherical relative positions [Shen et al. 2022] and spherical harmonics [Lee et al. 2025]. Recently, the focus has shifted towards scaling up data and transferring knowledge from perspective domains. DA<sup>2</sup> [Li et al. 2025] synthesizes panoramic training data via perspective-to-sphere projection and leverages perspective foundation models to generate high-quality pseudo-labels. In parallel, Depth Any Panoramas [Lin et al. 2025] establishes a metric depth foundation model through a data-in-the-loop paradigm. It constructs a large-scale dataset combining synthetic environments and real-world web data, and employs a DINOv3 [Siméoni et al. 2025] backbone with distortion-aware optimization to achieve robust zero-shot generalization without relying on explicit crop-based inference. Other works target specific modalities, such as PanoNormal [Huang et al. 2024a] for surface normal estimation and Open Panoramic Segmentation [Zheng et al. 2024] for semantic understanding. Despite these advances, most current methods operate as single-task specialists. The exploration of multi-task panoramic understanding is limited. [Guttikonda and Rambach 2024] utilizes multi-modal spherical inputs to assist semantic segmentation, yet their primary objective remains restricted to improving a single task rather than achieving holistic scene parsing, while [Huang et al. 2024b; Shah et al. 2024] is one of the few attempts to tackle multiple dense predictions on panoramas, but it relies on standard supervised learning and does not fully leverage the potential of modern foundation models or address the specific invariant vs. variant geometric conflicts between tasks.

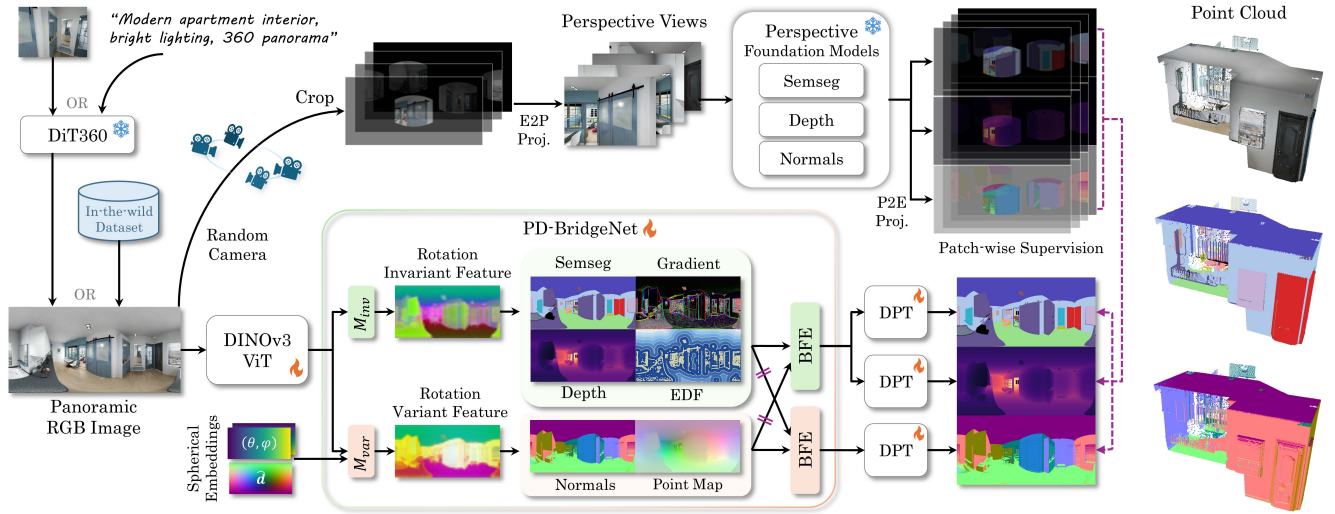


Fig. 2. **Overview of the MTPano framework.** We employ a label-free pipeline (top) that integrates dense priors from perspective foundation models via **patch-wise supervision**. We propose **PD-BridgeNet** (bottom), a dual-stream architecture that disentangles rotation-invariant and variant features via geometry-aware modulation ( $M_{inv}$  and  $M_{var}$ ). The streams are harmonized by a Truncated Gradient Flow mechanism, which facilitates synergistic information exchange while preventing optimization interference across branches. Auxiliary dense task supervisions are involved to aid the task interaction process: Image Gradient, Edge Distance Field (EDF), and Metric Point Map.

### 3 Method

In this section, we present **MTPano**, a unified framework for label-free multi-task panoramic scene understanding. To overcome the scarcity of annotations and inherent geometric conflicts, MTPano integrates two key components: a **Label-Free Training Pipeline** (Sec. A.2) that integrates dense priors from multiple perspective foundation models via randomized patch-wise supervision; and the **Panorama-Dual-BridgeNet** (Sec. 3.2), a dual-stream architecture that disentangles rotation-invariant and variant features via geometric modulation, and conduct feature interactions by a gradient-truncated bridge mechanism.

#### 3.1 Label-Free Training Pipeline

Our pipeline incorporates high-quality data collection/generation and pseudo-annotating from the perspective foundation models. We first collect annotation-free panoramic images from open-source datasets like [Xiao et al. 2012], in order to provide a higher diversity of data distribution, we also take advantage of current panorama generation methods like [Feng et al. 2025; Wang et al. 2023a] to synthesize a large quantity of indoor/outdoor panoramic scenes.

Despite this abundance of raw data, obtaining high-resolution, pixel-wise multi-task annotations remains prohibitively expensive. As shown in Fig. 2, to bypass this bottleneck, we leverage off-the-shelf perspective foundation models by transferring dense priors to the spherical domain via reciprocal projections. Given an unlabeled panorama  $I_{pano}$ , we generate  $N$  random perspective crops by sampling virtual camera poses with random FoV, yaw  $\psi_i$ , and pitch  $\eta_i$ . For each pose, we extract a perspective patch  $P_{persp}^i$  using

a task-aware P2E projection  $\Pi_{P2E}$ :

$$P_{persp}^i = \Pi_{P2E}(I_{pano}, \eta_i, \psi_i) = \begin{cases} I_{pano}(\mathbf{x}_s), & t = T_{sem}, \\ I_{pano}(\mathbf{x}_s) \cdot (\mathbf{d}_{cam} \cdot \mathbf{k}), & t = T_{depth}, \\ R(\eta_i, \psi_i)^{-1} \cdot I_{pano}(\mathbf{x}_s), & t = T_{norm}, \end{cases} \quad (1)$$

where  $\mathbf{x}_s$  denotes spherical coordinates,  $R$  is the rotation matrix, and  $\mathbf{d}_{cam} \cdot \mathbf{k}$  accounts for the projection angle relative to the optical axis. Since these patches are distortion-free, we directly apply InternImage-H [Wang et al. 2023b] and MoGe-2 [Wang et al. 2025c] to obtain high-quality dense predictions  $\hat{Y}_{persp}^i$ .

Directly stitching these predictions introduces significant artifacts due to scale inconsistencies. Instead, we propose a Patch-wise Supervision strategy. We re-project the pseudo-labels back to the spherical coordinate system using the inverse transform  $\hat{Y}_{patch}^i = \Pi_{E2P}(\hat{Y}_{persp}^i, \eta_i, \psi_i)$  (i.e., reversing Eq. 5 by dividing depth by  $\mathbf{d}_{cam} \cdot \mathbf{k}$  or rotating normals by  $R$ ). During training, we supervise the model using these patches and compute the loss only on valid pixels. This randomized supervision acts as a strong regularization, forcing the network to learn an average distribution consistent across varying views, effectively filtering out projection noise.

#### 3.2 Panorama-Dual-BridgeNet

While the data pipeline provides supervision, standard architectures struggle to handle the inherent ERP distortion and the geometric conflicts between tasks. To address this, we propose the **Panorama-Dual-BridgeNet (PD-BridgeNet)**. As illustrated in Fig. 3(c), our architecture is composed of three key components designed to progressively tame spherical features: (1) a **Geometric-Aware Disentanglement** module that splits features into rotation-invariant and -variant streams; (2) an **ERP Token Mixer** that adapts standard ViT features to the non-uniform spherical domain; and (3) a

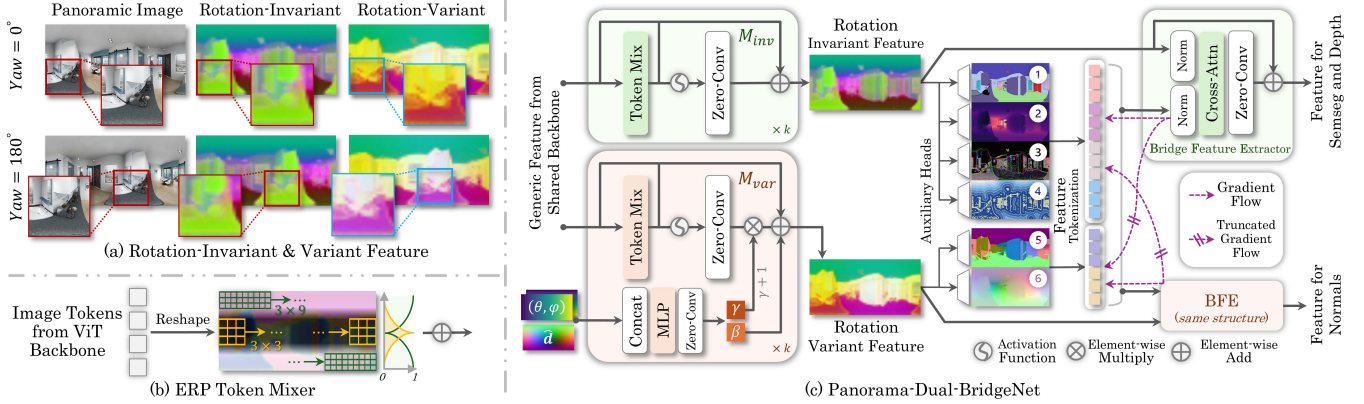


Fig. 3. (a) We classify dense prediction tasks into rotation-invariant (e.g., Semseg, Depth) and rotation-variant (e.g., Normal) groups based on their dependency on absolute observer orientation. The same region on the rotation-invariant feature remains consistent when rotation on the yaw angle is applied, while the rotation-variant feature doesn’t keep this consistency. (b) The **ERP Token Mixer** mitigates spherical distortion by dynamically fusing standard ( $3 \times 3$ ) and wide ( $3 \times 9$ ) kernels based on pixel latitude. (c) The proposed **Panorama-Dual-BridgeNet**. We disentangle feature learning into **Invariant** and **Variant** Stream via **Geometry Modulation** layers ( $M_{inv}$  and  $M_{var}$ ). The two streams are harmonized by a **Gradient-Truncated BridgeNet**, which aggregates initial predictions (Semantic Segmentation<sup>①</sup>, Depth<sup>②</sup>, Surface Normals<sup>③</sup>) with dense auxiliary cues (Image Gradient<sup>④</sup>, Edge Distance Field<sup>⑤</sup>, Point Map<sup>⑥</sup>) via Cross-Attention to provide thorough interactions while blocking the backward propagation of conflicting gradients.

**Gradient-Truncated Bridge** mechanism that facilitates safe cross-task interaction and avoid negative transfer.

### 3.2.1 Geometric-Aware Feature Disentanglement.

**Rotation-Invariant vs. Variant Features.** As illustrated in Fig. 3 (a), we first categorize dense prediction task features into two groups based on their geometric properties:

- **Rotation-Invariant Tasks ( $\mathcal{F}_{inv}$ ):** Tasks like semantic segmentation and depth depend on relative spatial context. Their values describe intrinsic object properties or distances relative to the camera center, which remain consistent regardless of the observer’s absolute orientation.
- **Rotation-Variant Tasks ( $\mathcal{F}_{var}$ ):** Tasks like surface normal estimation are strictly tied to the absolute coordinate system. Their values change strictly according to the camera’s viewing angle.

Sharing features naively between these conflicting groups leads to negative transfer. Therefore, we disentangle the feature processing into two parallel streams.

**Feature Disentanglement.** To effectively disentangle the conflicting task features defined above, we construct a dual-stream architecture. The **Invariant Stream ( $M_{inv}$ )** directly employs the ERP Token Mixer (introduced below) to aggregate spatial context. Since tasks in  $\mathcal{F}_{inv}$  (e.g., semantic segmentation) rely on intrinsic object properties and relative geometric relations, this stream focuses solely on extracting distortion-free visual representations without introducing directional or absolute positional priors.

In contrast, the **Variant Stream ( $M_{var}$ )** depends on absolute spherical coordinates to accurately predict rotation-sensitive attributes. The original features produced by self-supervised pre-trained backbones like DINO [Siméoni et al. 2025] are usually rich in consistent semantics but lack perceiving the absolute orientation of the viewer. To bridge this gap, we introduce a set of Spherical Embeddings by explicitly computing the normalized 3D ray direction  $\mathbf{d} \in \mathbb{R}^3$  for each pixel. For a spherical coordinate with

latitude  $\varphi$  and longitude  $\theta$ , the direction vector components are given by  $\mathbf{d} = [\cos \varphi \cos \theta, \sin \varphi, \cos \varphi \sin \theta]^T$ . We concatenate this directional vector  $\mathbf{d}$  with the positional embeddings of  $(\theta, \varphi)$  to form a condition vector, which is projected via a lightweight MLP to generate pixel-wise affine scale ( $\gamma$ ) and shift ( $\beta$ ) parameters. These parameters dynamically modulate the variant features via the Feature-wise Linear Modulation (FiLM) [Perez et al. 2018] layer:  $\mathcal{F}_{var} = (1 + \gamma) \cdot \mathcal{F}_{backbone} + \beta$ . This operation explicitly injects absolute sphere coordinate priors into the feature stream, breaking the spatial invariance and equipping the network with the necessary sense of direction to accurately predict rotation-variant properties like surface normals.

**ERP Token Mixer.** To support the dual-stream feature extraction on the sphere, the common challenge of distortion caused by Equirectangular Projection (ERP) needs to be handled. Standard convolutions or window partitioning fail on ERP images due to non-uniform pixel density (stretching at poles). As shown in Fig. 3 (b), we introduce an ERP Token Mixer to replace the standard convolution token mixer, which provides distortion-aware local features for the subsequent networks. As shown in Fig. 3 (b), for the feature tokens from the ViT backbone, we first reshape them back to the ERP domain, and the ERP Token Mixer applies a latitude-adaptive dual-kernel strategy:

$$\text{Mixer}(X) = (1 - w(\varphi)) \cdot (K_{3 \times 3} * X) + w(\varphi) \cdot (K_{3 \times 9} * X), \quad (2)$$

where  $K_{3 \times 3}$  handles equatorial regions, and the wide  $K_{3 \times 9}$  kernel accommodates polar stretching. The fusion weight  $w(\varphi) = |\sin(\varphi)|$  dynamically adjusts the receptive field based on latitude  $\varphi$ , ensuring uniform spatial aggregation across the sphere.

### 3.2.2 Gradient-Truncated Bridge Mechanism.

Independent processing of the two streams guarantees geometric purity but may lose synergistic information. To facilitate safe interaction, as shown in Fig. 3 (c), we design a bridge mechanism

Table 1. Comparisons of panoramic scene understanding on Structured3D, where \* indicates the method is trained on part of Structured3D training split.

Method	Semseg	Depth					Normals				
	<i>mIoU</i> ↑	<i>AbsRel</i> ↓	<i>RMSE</i> ↓	$\delta_1$ ↑	$\delta_2$ ↑	$\delta_3$ ↑	<i>Mean</i> ↓	<i>Median</i> ↓	< 11.5° ↑	< 22.5° ↑	< 30° ↑
Dinh et al. [Cao Dinh et al. 2024]	71.66	-	-	-	-	-	-	-	-	-	-
SFSS-MMSI [Guttikonda and Rambach 2024]	71.97	-	-	-	-	-	-	-	-	-	-
DAP* [Lin et al. 2025]	-	0.0341	0.1350	98.51	99.54	99.82	-	-	-	-	-
DA <sup>2s</sup> [Li et al. 2025]	-	0.0831	0.1600	95.71	98.00	98.77	-	-	-	-	-
PanDA* [Cao et al. 2025]	-	0.0379	0.1534	98.47	99.58	99.82	-	-	-	-	-
PanoNormal [Huang et al. 2024a]	-	-	-	-	-	-	5.562	0.1048	86.68	91.01	93.08
MultiPanoWise [Shah et al. 2024]	69.61	0.0557	0.1932	97.62	98.22	98.85	5.940	-	-	-	-
PanoFormer [Shen et al. 2022]	64.47	0.0861	0.3918	93.87	-	-	7.250	-	-	-	-
HUSH [Lee et al. 2025]	-	0.0459	0.2577	97.76	99.22	99.61	7.014	1.6380	83.40	89.90	92.60
InvPT [Ye and Xu 2022]	70.02	0.0421	0.1515	97.99	98.97	99.37	5.991	0.0822	87.81	91.18	92.71
BridgeNet [Zhang et al. 2025b]	70.13	0.0418	0.1492	98.17	99.01	99.42	5.988	0.0843	87.72	91.20	92.78
TaskPrompter [Ye and Xu 2023b]	70.95	0.0414	0.1428	98.33	99.38	99.65	5.962	0.0727	87.88	91.44	93.02
Ours	<b>75.66</b>	<b>0.0248</b>	<b>0.0968</b>	<b>99.27</b>	<b>99.74</b>	<b>99.87</b>	<b>3.850</b>	<b>0.0100</b>	<b>91.66</b>	<b>94.89</b>	<b>96.05</b>

Table 2. Comparisons of panoramic scene understanding on Stanford2D3D.

Method	Semseg	Depth					Normals				
	<i>mIoU</i> ↑	<i>AbsRel</i> ↓	<i>RMSE</i> ↓	$\delta_1$ ↑	$\delta_2$ ↑	$\delta_3$ ↑	<i>Mean</i> ↓	<i>Median</i> ↓	< 11.5° ↑	< 22.5° ↑	< 30° ↑
SFSS-MMSI [Guttikonda and Rambach 2024]	60.60	-	-	-	-	-	-	-	-	-	-
Trans4PASS [Zhang et al. 2024]	52.10	-	-	-	-	-	-	-	-	-	-
360BEV [Teng et al. 2024]	54.30	-	-	-	-	-	-	-	-	-	-
DAP [Lin et al. 2025]	-	0.0686	0.4662	95.64	98.71	99.34	-	-	-	-	-
DA <sup>2</sup> [Li et al. 2025]	-	<b>0.0616</b>	0.4261	<b>97.27</b>	<b>98.96</b>	99.36	-	-	-	-	-
PanDA [Cao et al. 2025]	-	0.0879	0.5989	93.96	98.56	99.33	-	-	-	-	-
MultiPanoWise [Shah et al. 2024]	54.60	0.0649	0.3892	94.51	-	-	-	-	-	-	-
HUSH [Lee et al. 2025]	-	0.0782	<b>0.3332</b>	93.84	98.49	99.29	11.191	3.8320	74.60	83.80	87.80
Dinh et al. [Cao Dinh et al. 2024]	55.50	0.1200	0.3900	86.50	98.80	99.10	-	-	-	-	-
InvPT [Ye and Xu 2022]	56.89	0.1207	0.5810	87.75	97.19	98.66	12.740	1.3920	76.34	82.87	85.26
BridgeNet [Zhang et al. 2025b]	57.12	0.1198	0.5834	87.97	97.38	98.92	12.840	1.4650	76.29	82.67	85.15
TaskPrompter [Ye and Xu 2023b]	57.55	0.1171	0.5792	88.29	97.50	99.06	12.390	1.3220	76.28	82.62	85.33
Ours	<b>69.47</b>	0.0675	0.4317	96.86	98.81	<b>99.37</b>	<b>9.706</b>	<b>0.9314</b>	<b>80.65</b>	<b>86.61</b>	<b>89.11</b>

supported by specific auxiliary supervision. This design serves a dual purpose: auxiliary tasks inject rich geometric and structural cues into the streams, while the truncated bridge ensures these features are shared for interactions without causing optimization conflicts.

**Dense Auxiliary Supervision.** To extract rich task-specific cues for the bridge, we introduce auxiliary tasks for each stream. For the Invariant Stream, we aim to incorporate low-level invariant priors (e.g., textures and boundaries) to aid high-level perception, a strategy validated by [Xu et al. 2018]. However, direct supervision on sparse edge pixels is inefficient for optimization. Instead, we propose two dense auxiliary tasks: (1) **Image Gradient Estimation**, which supervises the dense Sobel magnitude and direction; and (2) **Edge Distance Field (EDF)**, which predicts the unsigned distance field from each pixel to the nearest edge, providing global structural context. For the Variant Stream, to further enforce the understanding of absolute coordinate and global geometry, we introduce estimating **Metric Point Map**. This task requires the branch to predict the exact dense 3D coordinates  $(x, y, z)$  of the scene surface, explicitly aligning the feature space with the spherical spatial distribution.

**Bridge Feature Extraction.** We utilize lightweight auxiliary heads to generate predictions for these tasks. Intermediate features from these heads are extracted and flattened into tokens. To fuse these multi-source cues, we employ Bridge Feature Extractor (BFE) [Zhang et al. 2025b] based on Cross-Attention of each stream. The generic

backbone features act as *queries*, while the concatenated all task-specific features serve as *keys* and *values*. This aggregates complementary contexts into unified bridge features.

**Truncated Gradient Flow.** A critical challenge in this dual-stream interaction is the conflict between different feature attributes (invariant and variant), which leads to negative transfer during optimization. To mitigate this, we employ a Truncated Gradient Flow. By applying a detach operation to cross-stream features during aggregation, we enable the forward propagation of synergistic context while strictly blocking backward gradients from the opposing branch, effectively isolating optimization interference.

### 3.2.3 Optimization Strategy.

**Zero-Convolution & Progressive Warmup.** To effectively leverage the pre-trained DINOv3 backbone, we employ two stabilization strategies. First, we apply **Zero-Convolution** [Zhang et al. 2023b] to all injection layers. By initializing the injection weights to zero, the network starts as an identity mapping, preserving the foundation model’s priors while allowing task-specific refinements to be integrated progressively. Second, to prevent noise gradients from randomly initialized heads, we adopt a **Progressive Warmup** strategy. We first freeze the backbone and exclusively optimize the auxiliary heads to align projections with the feature distribution. Once stabilized, we unfreeze the full framework for end-to-end finetuning.

**Multi-Task Objective.** Following standard multi-task optimization protocols [Xu et al. 2018; Ye and Xu 2022; Zhang et al. 2025b], our total loss  $\mathcal{L}_{total}$  is a weighted sum of main task losses and auxiliary supervision losses. Crucially, to encourage the recovery of fine-grained high-frequency details for geometry tasks (depth and normals), we incorporate the geometry regularization from [Zhang et al. 2025a] into our objective:

$$\mathcal{L}_{total} = \sum_{t \in \mathcal{T}_{main}} \lambda_t \mathcal{L}_t + \sum_{t \in \mathcal{T}_{aux}} \lambda_t \mathcal{L}_t + \sum_{t \in \{T_d, T_n\}} \lambda_{geo} \mathcal{L}_{geo}. \quad (3)$$

## 4 Experiments

### 4.1 Experimental Settings

**Training Datasets.** We simulate a strictly unsupervised scenario by compiling a large-scale composite dataset and discarding all original ground-truth annotations. The training set consists of 140,884 panoramic images from four sources: 20,041 from Structured3D [Zheng et al. 2020], 34,260 from Sun360 [Xiao et al. 2012], 10,359 from Matterport3D [Chang et al. 2017], and 76,224 high-quality synthetic images generated by DiT360 [Feng et al. 2025]. For panoramas from all datasets mentioned above, we do not use their ground-truth labels if applicable; instead, we randomly sample  $N = 32$  perspective crops to ensure comprehensive spherical coverage. The sampling parameters are randomized as follows: Field-of-View (FoV)  $\in [80^\circ, 120^\circ]$ , Yaw  $\in [0^\circ, 360^\circ]$ , and Pitch  $\in [-90^\circ, 90^\circ]$ . The pseudo-labels for these crops are generated by off-the-shelf perspective foundation models: InternImage-H [Wang et al. 2023b] (pretrained on ADE20k [Zhou et al. 2019]) is used for semantic segmentation, while MoGe-2 [Wang et al. 2025c] provides geometry estimation (depth and surface normals). These perspective predictions are then re-projected onto the sphere to serve as patch-wise supervision for MTPano.

**Evaluation Datasets & Metrics.** We assess the efficacy of MTPano on two standard indoor panoramic benchmarks: **Structured3D [Zheng et al. 2020]** (synthetic) and **Stanford2D3D [Armeni et al. 2017]** (real-world). Following the experimental protocols outlined in [Guttikonda and Rambach 2024; Shah et al. 2024], we adopt their respective training and testing splits. Since MTPano inherits the output characteristics of perspective foundation models (e.g., ADE20k semantic categories and MoGe’s geometric scale), we finetune MTPano to adaptively align the prediction space with the evaluation benchmarks’ ground truth for valid comparison. We report standard dense prediction metrics: mean Intersection over Union (mIoU) for semantic segmentation; Absolute Relative error (AbsRel), RMSE, and  $\delta_n$  accuracies for depth; and Mean/Median angular error along with percentage of pixels within angular thresholds ( $11.5^\circ$ ,  $22.5^\circ$ ,  $30^\circ$ ) for surface normals.

**Implementation Details.** MTPano is implemented in PyTorch. We utilize the pre-trained DINOv3-Large [Siméoni et al. 2025] as the backbone and employ a DPT [Ranftl et al. 2021] head with an embedding dimension of 512 for dense predictions. The input resolution is set to  $512 \times 1024$ . The model is trained for 100,000 iterations using the Adam optimizer with a base learning rate of  $2 \times 10^{-5}$  and a weight decay of  $5 \times 10^{-6}$ . We use a polynomial learning rate scheduler with a power of 0.9. The batch size is set to 4 per GPU. The loss weights are set to  $\lambda_{sem} = \lambda_{depth} = \lambda_{norm} = 1.0$ ,

Table 3. Ablation study on Structured3D. We use DINOv3-Small for this experiment. STL for single-task learning and MTL for multi-task learning.

Method	Semseg	Depth	Normals	Delta MTL
	mIoU $\uparrow$	RMSE $\downarrow$	Mean $\downarrow$	$\Delta_{MTL}$ (%)
STL	64.21	0.1989	5.9120	+0.00
MTL baseline	65.17	0.1501	5.5220	+10.88
w.o. $M_{var}$ $M_{inv}$ $Trunc$	66.36	0.1437	5.4850	+12.77
w.o. $M_{var}$ $M_{inv}$	66.54	0.1434	5.4930	+12.87
w.o. Aux Heads	65.68	0.1435	5.4850	+12.46
Full MTPano	<b>66.64</b>	<b>0.1432</b>	<b>5.4740</b>	<b>+13.07</b>

for auxiliary tasks we set the weight to 0.003. To stabilize the dual-stream interaction, we apply the proposed progressive warmup for 1000 steps prior to end-to-end training. All experiments are conducted on 8 NVIDIA A100 GPUs.

### 4.2 Qualitative and Quantitative Evaluation

As shown in Tab. 1, on Structured3D, MTPano achieves state-of-the-art performance across all three tasks, consistently outperforming both single-task specialists and multi-task baselines. Specifically, it attains **75.66%** mIoU in semantic segmentation, surpassing the previous best SFSS-MMSI [Guttikonda and Rambach 2024] by **+3.69%**. In geometry estimation, our unified model outperforms dedicated specialists, reducing depth AbsRel to **0.0248** (vs. DAP’s 0.0341) and surface normal mean error to **3.85°** (vs. PanoNormal’s 5.56°). Notably, compared to standard panoramic MTL baselines like Taskprompter [Ye and Xu 2023b] and BridgeNet [Zhang et al. 2025b], MTPano reduces depth error by approximately **40%**, verifying that our PD-BridgeNet effectively handles task interactions on panoramic images. This performance trend extends to the real-world Stanford2D3D benchmark (Tab. 2). MTPano leads semantic segmentation with **69.47%** mIoU (**+8.87%** gain) and achieves a state-of-the-art normal mean error of **9.71°**. In depth estimation, despite a marginal deficit in AbsRel compared to the specialist  $DA^2$  [Li et al. 2025], MTPano still significantly outperforms all multi-task baselines, validating its robust geometric consistency in diverse domains.

Qualitative results in Fig. 4 demonstrate that MTPano yields significantly sharper predictions than SOTA specialists. Specifically, MTPano captures fine-grained boundaries more accurately than DAP [Lin et al. 2025] and PanoNormal [Huang et al. 2024a] (Fig. 4a), and recovers distortion-free 3D point clouds without the geometric noise observed in TaskPrompter [Ye and Xu 2023b] (Fig. 4b). Furthermore, Fig. 5 validates MTPano’s robust generalization on real-world Stanford2D3D data, maintaining high semantic and geometric fidelity despite domain gaps.

### 4.3 Ablation Study

We conduct comprehensive ablation studies on the Structured3D dataset to validate the effectiveness of the proposed components in MTPano. The results are summarized in Tab. 3 and Fig. 6.

**Effectiveness of PD-BridgeNet Components.** Following a standard in multi-task learning [Vandenhende et al. 2020], we adopt  $\Delta_{MTL}$  to indicate the average relative improvement over STL baselines. Tab. 3 validates the contribution of each component. Removing auxiliary heads (Row 5) leads to a performance drop, confirming the importance of multiple auxiliary dense priors. Furthermore, the

absence of geometric modulation or the Truncated Gradient mechanism (Rows 3 & 4) degrades results, indicating that naive feature sharing induces negative transfer between conflicting task attributes. Ultimately, the full MTPano achieves a peak gain of +13.07%, proving the necessity of disentangled yet interactive learning.

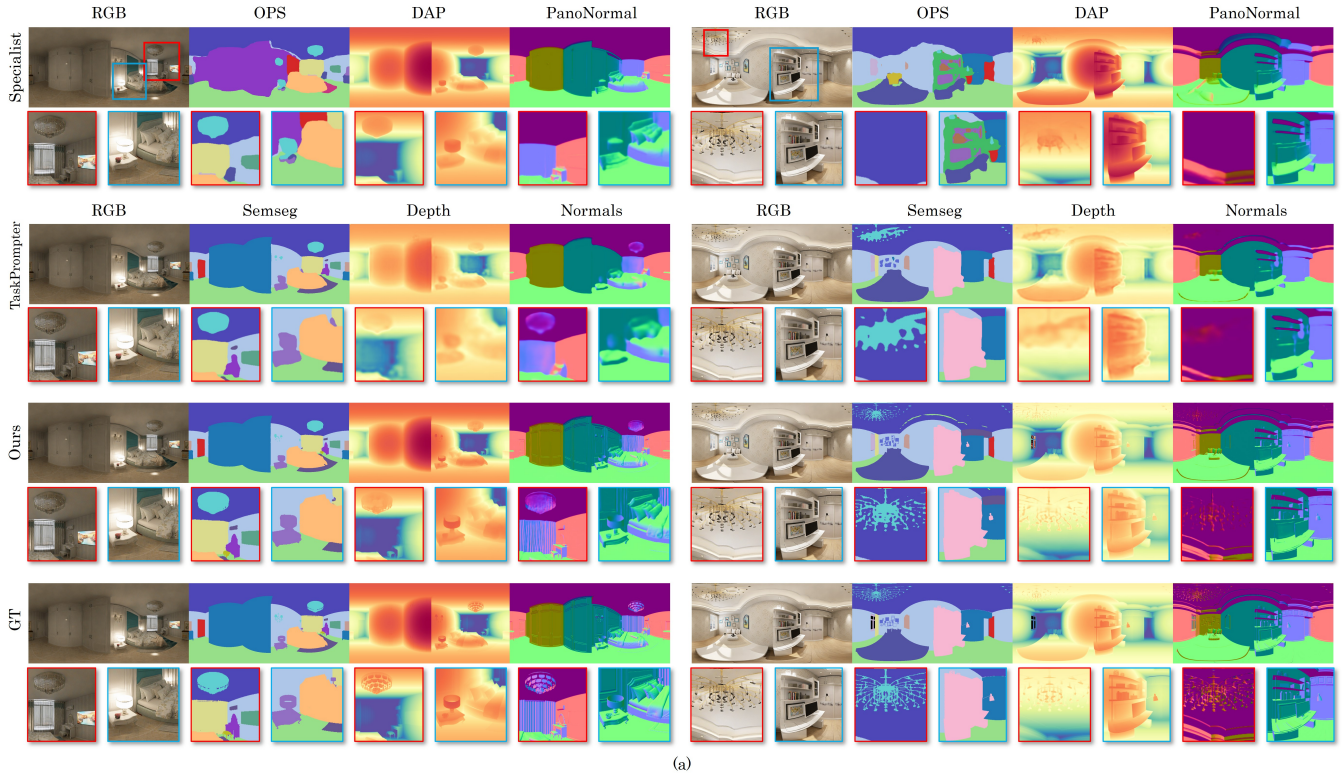
**Mutual Correction via Cross-Task Interaction.** A key advantage of our multi-task framework is its ability to correct noise inherent in the pseudo-labels. As illustrated in Fig. 6(a), the seaming artifacts and noise remains in the pseudo-ground truth (e.g., discontinuities in surface normals or depth). However, by jointly learning complementary tasks, MTPano leverages the consistency of one modality to refine another. For example, the global context from segmentation smooths out normal artifacts (Fig. 6(a) top row). Consequently, our model’s predictions are visually superior to the noisy pseudo-labels it was trained on, highlighting the robustness of the PD-BridgeNet in filtering projection noise through cross-task consensus.

**Visualizing Feature Disentanglement.** Fig. 6(b) visualizes feature maps under rotation. While shared backbone features ( $\mathcal{F}_{backbone}$ ) exhibit entangled attributes, our modulation layers enforce distinct behaviors: Invariant Features ( $\mathcal{F}_{inv}$ ) remain spatially stable and focus on high-level semantics, whereas Variant Features ( $\mathcal{F}_{var}$ ) capture orientation-sensitive cues that rotate with the camera. This confirmation of explicit disentanglement demonstrates the necessity of disentangling features with different attributes in PD-BridgeNet.

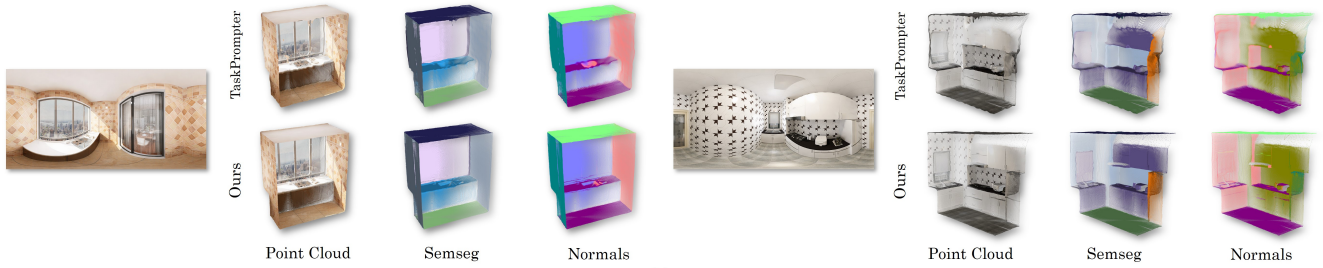
**Visualizing In-the-Wild Samples.** We visualize more samples in 7 generated by DiT360 [Feng et al. 2025] to test the generalize ability of MTPano. The semantic category is grounded on ADE20k for these samples. We provide 242 high-quality samples in the supplementary html.

## 5 Conclusion

We present MTPano, a label-free multi-task foundation model for panoramic scene understanding. By leveraging dense priors from perspective foundation models and introducing the PD-BridgeNet, our framework effectively disentangles rotation-invariant and -variant features while harmonizing their interaction via a truncated gradient mechanism. MTPano achieves state-of-the-art performance on several standard benchmarks, and demonstrates that unified multi-task learning offers a robust and scalable solution for high-fidelity panoramic scene understanding.



(a)



(b)

Fig. 4. **Qualitative comparisons on Structured3D.** (a) MTPano outperforms single-task specialists (OPS [Zheng et al. 2024], DAP [Lin et al. 2025], PanoNormal [Huang et al. 2024a]) and the multi-task baseline TaskPrompter [Ye and Xu 2023b], achieving superior segmentation accuracy and geometric detail via PD-BridgeNet’s interaction. (b) Point cloud reconstruction comparison demonstrating MTPano’s better structural consistency against TaskPrompter.

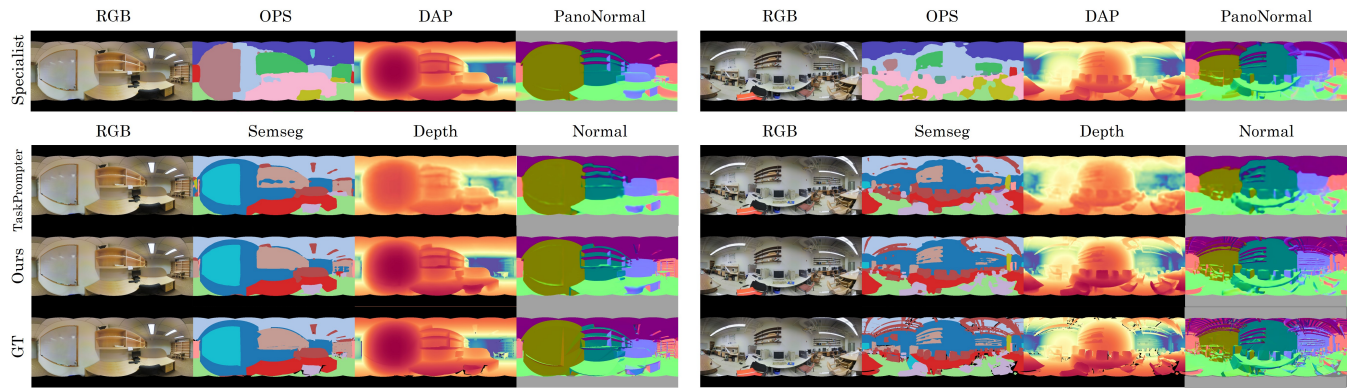


Fig. 5. **Qualitative comparisons with single task specialist models and multi-task models on Stanford2D3D.**

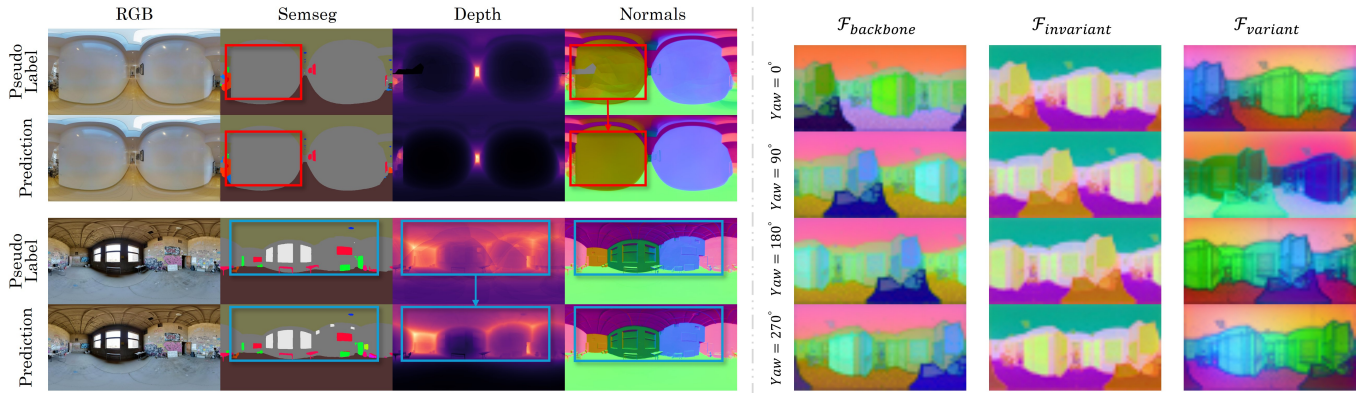


Fig. 6. **Analysis of cross-task learning and feature attributes.** (a) Multi-task interaction effectively eliminates projection artifacts in pseudo-labels. For instance, consistent semantic masks guide surface normal refinement (top), yielding predictions superior to the noisy supervision. (b) Feature visualization under rotation. While backbone features ( $\mathcal{F}_{backbone}$ ) exhibit entangled attributes, our approach successfully disentangles them into rotation-stable invariant features ( $\mathcal{F}_{ino}$ ) and orientation-sensitive variant features ( $\mathcal{F}_{var}$ ).

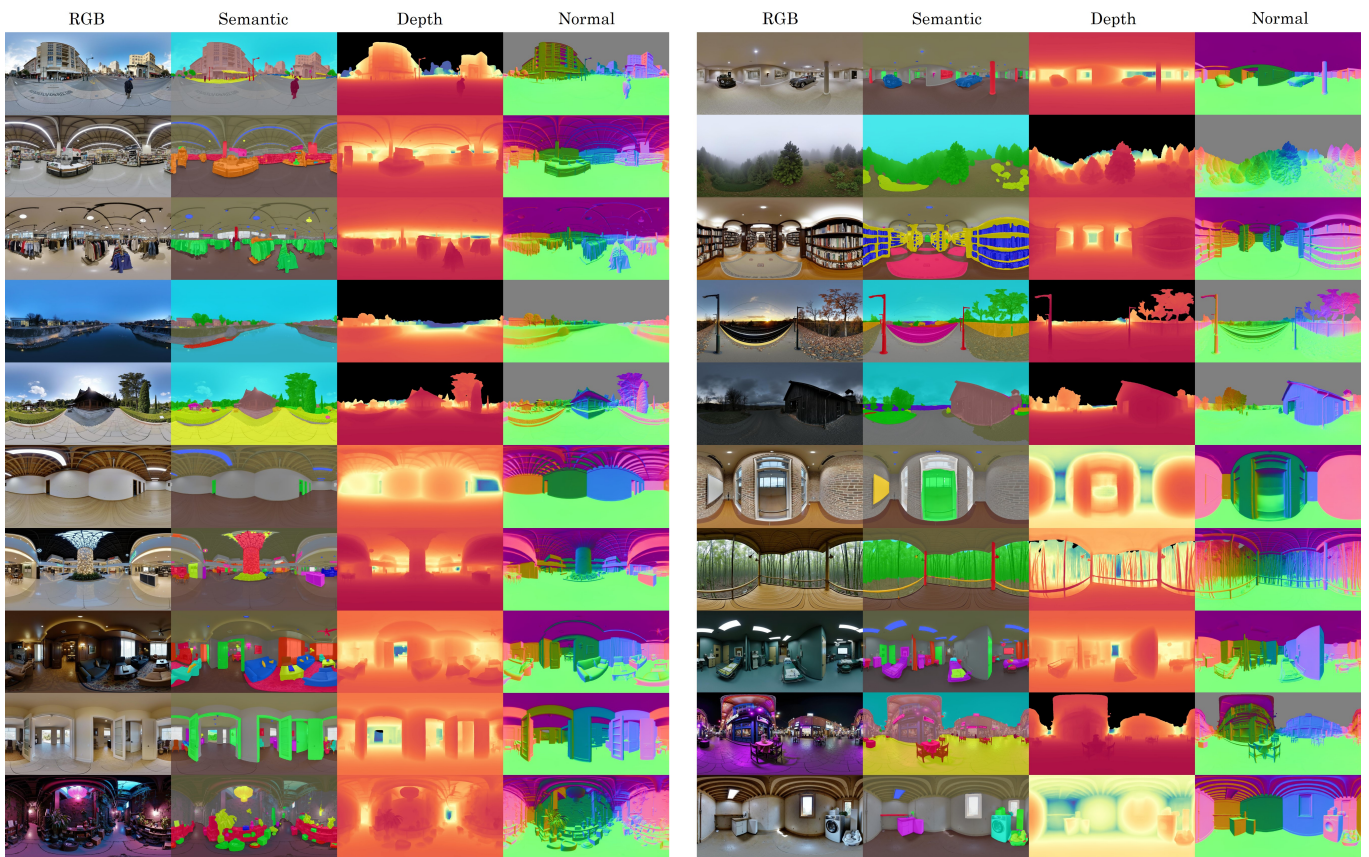


Fig. 7. **Visualization of in-the-wild panoramic scene understanding.**

## Supplementary Material

In this supplementary material, we provide additional implementation details regarding our data generation pipeline, the specific algorithms used for auxiliary task label generation, and further qualitative results demonstrating the generalization capabilities of MTPano.

### A Method Details

#### A.1 Data Generation Pipeline

To construct a large-scale, diverse, and high-fidelity training dataset without relying on limited real-world captures, we establish a synthetic data generation pipeline utilizing the DiT360 [Feng et al. 2025] framework. As shown in the provided script, our pipeline consists of two stages: attribute-based prompt engineering and multi-GPU batch generation.

*Attribute-Based Prompt Engineering.* To ensure the synthesized dataset covers a wide distribution of scene types and lighting conditions, we construct a comprehensive *Attribute Pool* derived from the distributions of SUN360 [Xiao et al. 2012] and Matterport3D [Chang et al. 2017]. The generation process is governed by a probabilistic template engine:

- **Hierarchical Scene Categorization:** We construct a diverse dictionary of scene attributes categorized into *Indoor* (covering Residential, Commercial, Public Spaces, and Industrial interiors) and *Outdoor* (covering Urban, Nature, Rural, and Historical sites) domains. For each generation task, we sample a scene category (e.g., “modern kitchen”, “dense pine forest”) with a weighted probability (60% Indoor, 40% Outdoor) to mimic the distribution of real-world applications.
- **Probabilistic Modifier Injection:** To prevent visual monotony, we inject three types of modifiers, each with a 50% independent trigger probability:
  - (1) *Lighting Conditions:* Modifies the global atmosphere (e.g., “golden hour sunset”, “cinematic lighting”, “blue hour twilight”).
  - (2) *Material & Texture Details:* Adds fine-grained object descriptions (e.g., “wooden flooring”, “exposed brick walls”, “lush vegetation”).
  - (3) *Quality Modifiers:* Enforces high-fidelity generation (e.g., “8k”, “photorealistic”, “masterpiece”).
- **Template Construction:** The final prompt  $P$  is assembled using a dynamic template structure:

$$P = \text{“A } [L] \text{ view of a } [S] \text{ with } [D], [Q], \text{ 360 panorama.”} \quad (4)$$

where  $[S]$  is the mandatory scene description, while  $[L]$  (Lighting),  $[D]$  (Details), and  $[Q]$  (Quality) are optional slots filled based on the Bernoulli trials described above. As shown in Fig. 8, we randomly pick some samples to show the distribution of synthetic data.

*Batch Generation.* We utilize the DiT360 pipeline [Feng et al. 2025], which leverages the FLUX.1-dev model equipped with panorama-specific LoRA adapters (Rank=128) for inference. To maximize throughput for the 140,884 images, we deploy a multi-process distributed generation system on 8×NVIDIA A100 (80GB) GPUs.

- **Inference Configuration:** We perform generation at a high resolution of  $2048 \times 1024$ . The denoising process is set to **35 inference steps** with a **Guidance Scale (CFG) of 3.0**, which we empirically found to yield the optimal balance between prompt adherence and visual fidelity.
- **Efficiency:** The pipeline operates in `float16` precision with a batch size of 4 per GPU. We assign a unique random seed to each sample to ensure diversity and employ a distributed task scheduler to handle job allocation and failure recovery robustly.

#### A.2 Label-Free Training Pipeline

Our pipeline incorporates high-quality data collection/generation and pseudo-annotating from the perspective foundation models. We first collect annotation-free panoramic images from open-source

Obtaining high-resolution, pixel-wise multi-task annotations for panoramic images is prohibitively expensive. To bypass this bottleneck, we leverage the rich knowledge encapsulated in off-the-shelf perspective foundation models by transferring dense priors to the spherical domain via reciprocal Perspective-to-Equirectangular (P2E) and Equirectangular-to-Perspective (E2P) projections.

Given an unlabeled panoramic image  $I_{pano}$ , we generate a set of random perspective crops. Specifically, we sample  $N$  virtual camera poses with random Field-of-Views (FoV), yaw  $\{\psi_i\}_1^N$ , and pitch  $\{\eta_i\}_1^N$  angles. For each pose, we extract a perspective patch  $P_{persp}^i$  using the standard P2E projection  $\Pi_{P2E}$ :

$$P_{persp}^i = \Pi_{P2E}(I_{pano}, \eta_i, \psi_i) = \begin{cases} I_{pano}(\mathbf{x}_s), & \text{if } t = T_{sem}, \\ I_{pano}(\mathbf{x}_s) \cdot (\mathbf{d}_{cam} \cdot \mathbf{k}), & \text{if } t = T_{depth}, \\ R(\eta_i, \psi_i)^{-1} \cdot I_{pano}(\mathbf{x}_s), & \text{if } t = T_{normal}, \end{cases} \quad (5)$$

where  $\mathbf{x}_s$  denotes the spherical coordinates in the panoramic domain,  $R(\eta_i, \psi_i)$  is the rotation matrix determined by the camera yaw  $\psi_i$  and pitch  $\eta_i$ .  $\mathbf{d}_{cam} \in \mathbb{R}^3$  indicates the normalized ray direction of  $\mathbf{x}_p$  in the local camera coordinate system, and  $\mathbf{k} = [0, 0, 1]^T$  represents the principal optical axis unit vector. Since these patches  $P_{persp}^i$  are distortion-free, we can directly apply powerful perspective foundation models to generate high-quality pseudo-labels. We utilize InternImage-H [Wang et al. 2023b] for semantic segmentation and MoGe-2 [Wang et al. 2025c] for geometry estimation (depth and normals), obtaining a set of dense predictions  $\hat{Y}_{persp}^i$ .

A naive approach would be to stitch these perspective predictions back into a full panoramic pseudo-label map. However, we empirically observe that stitching introduces significant artifacts, since the generated pseudo labels usually contain noise due to scale inconsistencies between overlapping crops, which could cause the model to overfit to the stitching patterns. Instead, we propose a **Patch-wise Supervision** strategy. We re-project the perspective pseudo-labels back to the spherical coordinate system using the

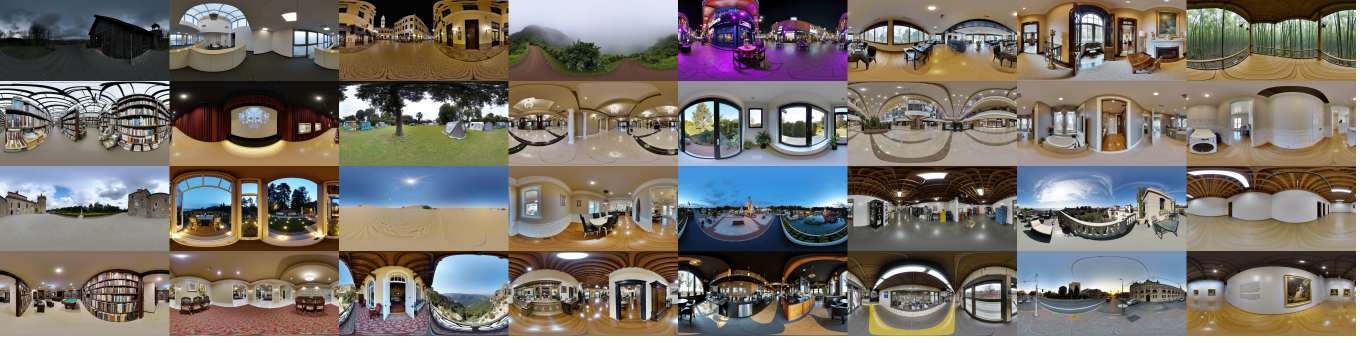


Fig. 8. Synthetic data generated by DiT360 [Feng et al. 2025].

inverse transform  $\Pi_{E2P}$ :

$$\begin{aligned} \hat{Y}_{patch}^i &= \Pi_{E2P}(\hat{Y}_{persp}^i, \eta_i, \psi_i) \\ &= \begin{cases} \hat{Y}_{persp}^i(\mathbf{x}_p), & \text{if } t = T_{sem}, \\ \hat{Y}_{persp}^i(\mathbf{x}_p), & \text{if } t = T_{depth}, \\ R(\eta_i, \psi_i) \cdot \hat{Y}_{persp}^i(\mathbf{x}_p), & \text{if } t = T_{normal}. \end{cases} \end{aligned} \quad (6)$$

where  $\mathbf{x}_p$  represents the pixel coordinates in the perspective patch. During training, we supervise the MTPano model using these pseudo label patches directly. We define a valid mask for each patch to compute the loss only on valid pixels. This randomized patch-level supervision acts as a strong regularization: it forces the network to learn an average distribution consistent across varying views, effectively filtering out noise and preventing overfitting to specific projection biases.

### A.3 Dense Auxiliary Supervision

To facilitate cross-task interaction in the PD-BridgeNet, we generate three types of dense auxiliary labels: Image Gradient, Edge Distance Field (EDF), and Metric Point Map. All computations are performed in a fully vectorized manner on the GPU to ensure efficiency.

*Image Gradient.* We compute the image gradient to provide low-level high-frequency cues (e.g., texture and boundaries) for the Rotation-Invariant stream. We first convert the RGB image to grayscale and apply a standard Sobel operator in the tensor space to obtain gradients  $G_x$  and  $G_y$ . The gradient magnitude  $M$  and direction  $\Phi$  are computed as:

$$M = \sqrt{G_x^2 + G_y^2}, \quad \Phi = \text{atan2}(G_y, G_x). \quad (7)$$

For visualization and supervision, we map the direction  $\Phi$  to the Hue channel and the magnitude  $M$  to the Value channel in the HSV color space.

*Edge Distance Field (EDF).* The EDF provides global structural context by encoding the distance from each pixel to the nearest edge. We implement this using the **Jump Flooding Algorithm (JFA)** [Rong and Tan 2006], which allows for parallel distance transform computation on the GPU. The process is as follows:

- (1) **Edge Extraction:** We derive a binary edge mask  $B$  from the image gradient magnitude using a high threshold ( $\tau = 0.99$ ).

To prevent the SDF from collapsing at image boundaries, we explicitly clear the border regions of the mask.

- (2) **JFA Distance Transform:** We initialize a seed map where edge pixels store their own coordinates and background pixels store an infinite value. The JFA iteratively propagates the coordinates of the nearest seed with a step size decaying from  $N/2$  to 1.
- (3) **Distance Calculation:** The final EDF map is obtained by calculating the Euclidean distance between each pixel coordinate and its stored nearest seed coordinate.

*Metric Point Map.* To explicitly align the feature space with the spherical spatial distribution for the Rotation-Variant stream, we generate a Metric Point Map. This map represents the absolute 3D coordinate  $(x, y, z)$  of the scene surface for each pixel. Given the metric depth map  $D \in \mathbb{R}^{H \times W}$  (derived from MoGe-2 [Wang et al. 2025c]), we first generate the spherical unit ray direction map  $\mathbf{r} \in \mathbb{R}^{3 \times H \times W}$ . For a pixel  $(u, v) \in [-1, 1]^2$ , the spherical coordinates are  $\theta = u\pi$ ,  $\phi = v\frac{\pi}{2}$ , and the Cartesian unit vector is:

$$\mathbf{r}(u, v) = [\cos \phi \sin \theta, \sin \phi, -\cos \phi \cos \theta]^T. \quad (8)$$

The final Metric Point Map is computed as  $\mathbf{P} = D \odot \mathbf{r}$ . We store these maps in 16-bit integer format (scaled to millimeters) to preserve precision during training.

## B More Visualized Results

We show more comparisons with SoTA methods in Fig. 9. We present extensive additional qualitative results in the accompanying supplementary webpage (HTML). We provide a gallery of 242 diverse samples from our synthetic dataset and in-the-wild captures, showcasing MTPano’s robust performance across semantic segmentation, depth estimation, and surface normal prediction in varied lighting and scene conditions. Readers are encouraged to browse the HTML file for a comprehensive assessment of the visual quality and cross-task consistency. We randomly picked some of them in Fig. 10.

## References

- Iro Armeni, Sasha Sax, Amir R Zamir, and Silvio Savarese. 2017. Joint 2d-3d-semantic data for indoor scene understanding. *arXiv preprint arXiv:1702.01105* (2017).
- Yancheng Cai, Bo Zhang, Baopu Li, Tao Chen, Hongliang Yan, Jingdong Zhang, and Jiahao Xu. 2023. Rethinking cross-domain pedestrian detection: A background-focused distribution alignment framework for instance-free one-stage detectors. *IEEE transactions on image processing* 32 (2023), 4935–4950.

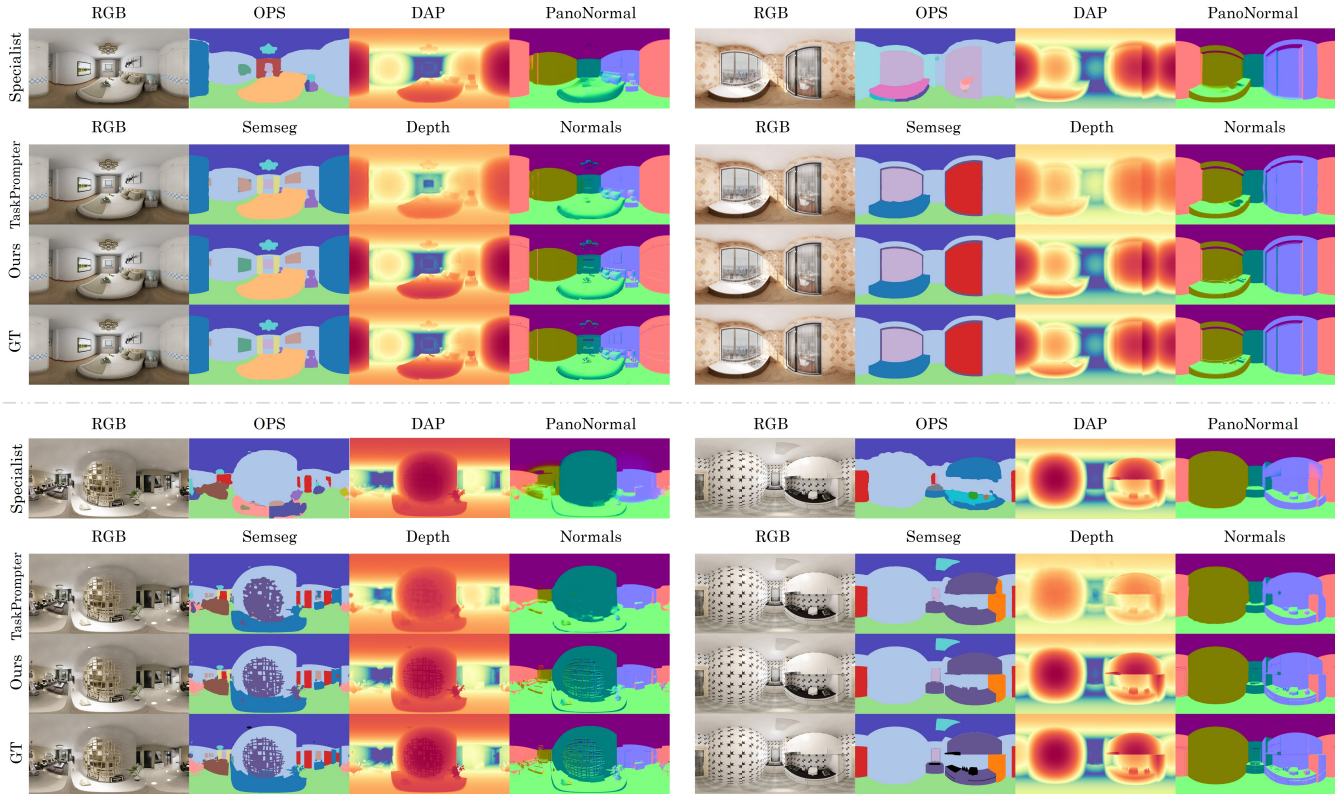


Fig. 9. More qualitative comparisons with on Structured3D.

Mang Cao, Sanping Zhou, Ye Deng, Wenli Huang, Le Wang, and Jinjun Wang. [n. d.]. MSM: Multi-Scale Mamba in Multi-Task Dense Prediction. ([n. d.]).

Zidong Cao, Jinjing Zhu, Weiming Zhang, Hao Ai, Haotian Bai, Hengshuang Zhao, and Lin Wang. 2025. PanDA: Towards Panoramic Depth Anything with Unlabeled Panoramas and Mobius Spatial Augmentation. In *Proceedings of the Computer Vision and Pattern Recognition Conference*. 982–992.

Duc Cao Dinh, Seok Joon Kim, and Kyusung Cho. 2024. Geometric exploitation for indoor panoramic semantic segmentation. *Advances in Neural Information Processing Systems* 37 (2024), 26355–26376.

Angel Chang, Angela Dai, Thomas Funkhouser, Maciej Halber, Matthias Niessner, Manolis Savva, Shuran Song, Andy Zeng, and Yinda Zhang. 2017. Matterport3d: Learning from rgb-d data in indoor environments. *arXiv preprint arXiv:1709.06158* (2017).

Ruchika Chavhan, Abhinav Mehrotra, Malcolm Chadwick, Alberto Gil Ramos, Luca Morreale, Mehdi Noroozi, and Sourav Bhattacharya. 2025. Upcycling Text-to-Image Diffusion Models for Multi-Task Capabilities. *arXiv preprint arXiv:2503.11905* (2025).

Alexey Dosovitskiy, Lucas Beyer, Alexander Kolesnikov, Dirk Weissenborn, Xiaohua Zhai, Thomas Unterthiner, Mostafa Dehghani, Matthias Minderer, Georg Heigold, Sylvain Gelly, et al. 2020. An image is worth 16x16 words: Transformers for image recognition at scale. *arXiv preprint arXiv:2010.11929* (2020).

Haoran Feng, Dizhe Zhang, Xiangtai Li, Bo Du, and Lu Qi. 2025. Dit360: High-fidelity panoramic image generation via hybrid training. *arXiv preprint arXiv:2510.11712* (2025).

Xiao Fu, Wei Yin, Mu Hu, Kaixuan Wang, Yuexin Ma, Ping Tan, Shaojie Shen, Dahua Lin, and Xiaoxiao Long. 2024. Geowizard: Unleashing the diffusion priors for 3d geometry estimation from a single image. In *European Conference on Computer Vision*. Springer, 241–258.

Yuan Gao, Jiayi Ma, Mingbo Zhao, Wei Liu, and Alan L Yuille. 2019. Nddr-cnn: Layerwise feature fusion in multi-task cnns by neural discriminative dimensionality reduction. In *CVPR*. 3205–3214.

Suresh Guttikonda and Jason Rambach. 2024. Single frame semantic segmentation using multi-modal spherical images. In *Proceedings of the IEEE/CVF Winter Conference on Applications of Computer Vision*. 3222–3231.

Kaiming He, Xinlei Chen, Saining Xie, Yanghao Li, Piotr Dollár, and Ross Girshick. 2022. Masked autoencoders are scalable vision learners. In *Proceedings of the IEEE/CVF*

*conference on computer vision and pattern recognition*. 16000–16009.

Mu Hu, Wei Yin, Chi Zhang, Zhipeng Cai, Xiaoxiao Long, Hao Chen, Kaixuan Wang, Gang Yu, Chunhua Shen, and Shaojie Shen. 2024. Metric3d v2: A versatile monocular geometric foundation model for zero-shot metric depth and surface normal estimation. *IEEE Transactions on Pattern Analysis and Machine Intelligence* (2024).

Kun Huang, Fanglue Zhang, and Neil A Dodgson. 2024a. PanoNormal: Monocular Indoor 360° Surface Normal Estimation. Available at SSRN 5100169 (2024).

Kun Huang, Fang-Lue Zhang, Fangfang Zhang, Yu-Kun Lai, Paul L Rosin, and Neil A Dodgson. 2024b. Multi-task Geometric Estimation of Depth and Surface Normal from Monocular 360 { \deg } Images. *arXiv preprint arXiv:2411.01749* (2024).

Bingxin Ke, Anton Obukhov, Shengyu Huang, Nando Metzger, Rodrigo Caye Daudt, and Konrad Schindler. 2024. Repurposing diffusion-based image generators for monocular depth estimation. In *Proceedings of the IEEE/CVF conference on computer vision and pattern recognition*. 9492–9502.

Alexander Kirillov, Eric Mintun, Nikhila Ravi, Hanzi Mao, Chloe Rolland, Laura Gustafson, Tete Xiao, Spencer Whitehead, Alexander C Berg, Wan-Yen Lo, et al. 2023. Segment anything. In *Proceedings of the IEEE/CVF international conference on computer vision*. 4015–4026.

Iro Laina, Christian Rupprecht, Vasileios Belagiannis, Federico Tombari, and Nassir Navab. 2016. Deeper depth prediction with fully convolutional residual networks. In *2016 Fourth international conference on 3D vision (3DV)*. IEEE, 239–248.

Jongsung Lee, Harin Park, Byeong-Uk Lee, and Kyungdon Joo. 2025. HUSH: Holistic Panoramic 3D Scene Understanding using Spherical Harmonics. In *Proceedings of the Computer Vision and Pattern Recognition Conference*. 16599–16608.

Haodong Li, Wangguangdong Zheng, Jing He, Yuhao Liu, Xin Lin, Xin Yang, Ying-Cong Chen, and Chunchao Guo. 2025. DA<sup>2</sup>: Depth Anything in Any Direction. *arXiv preprint arXiv:2509.26618* (2025).

Wei-Hong Li, Steven McDonagh, Ales Leonardis, and Hakan Bilen. 2023. Multi-task learning with 3d-aware regularization. *arXiv preprint arXiv:2310.00986* (2023).

Xin Lin, Meixi Song, Dizhe Zhang, Wenxuan Lu, Haodong Li, Bo Du, Ming-Hsuan Yang, Truong Nguyen, and Lu Qi. 2025. Depth Any Panoramas: A Foundation Model for Panoramic Depth Estimation. *arXiv preprint arXiv:2512.16913* (2025).

Shikun Liu, Edward Johns, and Andrew J Davison. 2019. End-to-end multi-task learning with attention. In *CVPR*. 1871–1880.

- Yuxiang Lu, Shengcao Cao, and Yu-Xiong Wang. 2024. Swiss army knife: Synergizing biases in knowledge from vision foundation models for multi-task learning. *arXiv preprint arXiv:2410.14633* (2024).
- Ishan Misra, Abhinav Shrivastava, Abhinav Gupta, and Martial Hebert. 2016. Cross-stitch networks for multi-task learning. In *CVPR*. 3994–4003.
- Maxime Oquab, Timothée Darcet, Théo Moutakanni, Huy Vo, Marc Szafraniec, Vasil Khalidov, Pierre Fernandez, Daniel Haziza, Francisco Massa, Alaaeldin El-Nouby, et al. 2023. Dinov2: Learning robust visual features without supervision. *arXiv preprint arXiv:2304.07193* (2023).
- Songyou Peng, Kyle Genova, Chiyu Jiang, Andrea Tagliasacchi, Marc Pollefeys, Thomas Funkhouser, et al. 2023. Openscene: 3d scene understanding with open vocabularies. In *Proceedings of the IEEE/CVF conference on computer vision and pattern recognition*. 815–824.
- Ethan Perez, Florian Strub, Harm De Vries, Vincent Dumoulin, and Aaron Courville. 2018. Film: Visual reasoning with a general conditioning layer. In *Proceedings of the AAAI conference on artificial intelligence*, Vol. 32.
- René Ranftl, Alexey Bochkovskiy, and Vladlen Koltun. 2021. Vision transformers for dense prediction. In *Proceedings of the IEEE/CVF international conference on computer vision*. 12179–12188.
- Tianhe Ren, Yihao Chen, Qing Jiang, Zhaoyang Zeng, Yuda Xiong, Wenlong Liu, Zhengyu Ma, Junyi Shen, Yuan Gao, Xiaohe Jiang, et al. 2024. Dino-x: A unified vision model for open-world object detection and understanding. *arXiv preprint arXiv:2411.14347* (2024).
- Guodong Rong and Tiow-Seng Tan. 2006. Jump flooding in GPU with applications to Voronoi diagram and distance transform. In *Proceedings of the 2006 symposium on Interactive 3D graphics and games*. 109–116.
- Uzair Shah, Muhammad Tukur, Mahmood Alzubaidi, Giovanni Pintore, Enrico Gobbetti, Mowafa Househ, Jens Schneider, and Marco Agus. 2024. MultiPanoWise: holistic deep architecture for multi-task dense prediction from a single panoramic image. In *Proceedings of the IEEE/CVF Conference on Computer Vision and Pattern Recognition*. 1311–1321.
- Zhijie Shen, Chunyu Lin, Kang Liao, Lang Nie, Zishuo Zheng, and Yao Zhao. 2022. PanoFormer: Panorama Transformer for Indoor 360° Depth Estimation. In *European Conference on Computer Vision*. Springer, 195–211.
- Oriane Siméoni, Huy V Vo, Maximilian Seitzer, Federico Baldassarre, Maxime Oquab, Cijo Jose, Vasil Khalidov, Marc Szafraniec, Seungeun Yi, Michaël Ramamonjisoa, et al. 2025. Dinov3. *arXiv preprint arXiv:2508.10104* (2025).
- Yingjie Tang, Shou Feng, Chunhui Zhao, Yongqi Chen, Zhiyong Lv, and Weiwei Sun. 2025. A Semantic Change Detection Network Based on Boundary Detection and Task Interaction for High-Resolution Remote Sensing Images. *IEEE Transactions on Neural Networks and Learning Systems* (2025).
- Zhifeng Teng, Jiaming Zhang, Kailun Yang, Kunyu Peng, Hao Shi, Simon Reiß, Ke Cao, and Rainer Stiefelhagen. 2024. 360bev: Panoramic semantic mapping for indoor bird’s-eye view. In *Proceedings of the IEEE/CVF Winter Conference on Applications of Computer Vision*. 373–382.
- Yuxin Tian, Yijie Lin, Qing Ye, Jian Wang, Xi Peng, and Jiancheng Lv. 2024. UNITE: multitask learning with sufficient feature for dense prediction. *IEEE Transactions on Systems, Man, and Cybernetics: Systems* 54, 8 (2024), 5012–5024.
- Simon Vandenhende, Stamatios Georgoulis, and Luc Van Gool. 2020. Mti-net: Multi-scale task interaction networks for multi-task learning. In *ECCV*. Springer, 527–543.
- Jionghao Wang, Ziyu Chen, Jun Ling, Rong Xie, and Li Song. 2023a. 360-degree panorama generation from few unregistered nfov images. *arXiv preprint arXiv:2308.14686* (2023).
- Ruicheng Wang, Sicheng Xu, Cassie Dai, Jianfeng Xiang, Yu Deng, Xin Tong, and Jiaolong Yang. 2025b. Moge: Unlocking accurate monocular geometry estimation for open-domain images with optimal training supervision. In *Proceedings of the Computer Vision and Pattern Recognition Conference*. 5261–5271.
- Ruicheng Wang, Sicheng Xu, Yue Dong, Yu Deng, Jianfeng Xiang, Zelong Lv, Guangzhong Sun, Xin Tong, and Jiaolong Yang. 2025c. MoGe-2: Accurate Monocular Geometry with Metric Scale and Sharp Details. *arXiv preprint arXiv:2507.02546* (2025).
- Wenhao Wang, Jifeng Dai, Zhe Chen, Zhenhang Huang, Zhiqi Li, Xizhou Zhu, XiaoWei Hu, Tong Lu, Lewei Lu, Hongsheng Li, et al. 2023b. Internimage: Exploring large-scale vision foundation models with deformable convolutions. In *Proceedings of the IEEE/CVF conference on computer vision and pattern recognition*. 14408–14419.
- Xiaoye Wang, Chen Tang, Xiangyu Yue, and Wei-Hong Li. 2025a. 3D-Aware Multi-Task Learning with Cross-View Correlations for Dense Scene Understanding. *arXiv preprint arXiv:2511.20646* (2025).
- Jianxiong Xiao, Krista A Ehinger, Aude Oliva, and Antonio Torralba. 2012. Recognizing scene viewpoint using panoramic place representation. In *2012 IEEE conference on computer vision and pattern recognition*. IEEE, 2695–2702.
- Dan Xu, Wanli Ouyang, Xiaogang Wang, and Nicu Sebe. 2018. Pad-net: Multi-tasks guided prediction-and-distillation network for simultaneous depth estimation and scene parsing. In *CVPR*. 675–684.
- Lihe Yang, Bingyi Kang, Zilong Huang, Xiaogang Xu, Jiashi Feng, and Hengshuang Zhao. 2024a. Depth anything: Unleashing the power of large-scale unlabeled data. In *Proceedings of the IEEE/CVF conference on computer vision and pattern recognition*. 10371–10381.
- Lihe Yang, Bingyi Kang, Zilong Huang, Zhen Zhao, Xiaogang Xu, Jiashi Feng, and Hengshuang Zhao. 2024b. Depth anything v2. *Advances in Neural Information Processing Systems* 37 (2024), 21875–21911.
- Nan Yang, Lukas von Stumberg, Rui Wang, and Daniel Cremers. 2020. D3vo: Deep depth, deep pose and deep uncertainty for monocular visual odometry. In *CVPR*. 1281–1292.
- Siwei Yang, Hanrong Ye, and Dan Xu. 2023. Contrastive multi-task dense prediction. In *Proceedings of the AAAI Conference on Artificial Intelligence (AAAI)*.
- Yuqi Yang, Peng-Tao Jiang, Qibin Hou, Hao Zhang, Jinwei Chen, and Bo Li. [n. d.]. Multi-Task Dense Predictions via Unleashing the Power of Diffusion. In *The Thirteenth International Conference on Learning Representations*.
- Hanrong Ye and Dan Xu. 2022. Inverted Pyramid Multi-task Transformer for Dense Scene Understanding. *ECCV* (2022).
- Hanrong Ye and Dan Xu. 2023a. TaskExpert: Dynamically Assembling Multi-Task Representations with Memorial Mixture-of-Experts. In *Proceedings of the IEEE/CVF International Conference on Computer Vision*. 21828–21837.
- Hanrong Ye and Dan Xu. 2023b. TaskPrompter: Spatial-Channel Multi-Task Prompting for Dense Scene Understanding. In *ICLR*.
- Hanrong Ye and Dan Xu. 2024. DiffusionMTL: Learning Multi-Task Denoising Diffusion Model from Partially Annotated Data. In *CVPR*.
- Wei Yin, Chi Zhang, Hao Chen, Zhipeng Cai, Gang Yu, Kaixuan Wang, Xiaozhi Chen, and Chunhua Shen. 2023. Metric3d: Towards zero-shot metric 3d prediction from a single image. In *Proceedings of the IEEE/CVF international conference on computer vision*. 9043–9053.
- Jingdong Zhang, Weikai Chen, Yuan Liu, Jionghao Wang, Zhengming Yu, Zhuowen Shen, Bo Yang, Wenping Wang, and Xin Li. 2025a. SPGen: Spherical Projection as Consistent and Flexible Representation for Single Image 3D Shape Generation. In *Proceedings of the SIGGRAPH Asia 2025 Conference Papers*. 1–12.
- Jingdong Zhang, Jiayuan Fan, Peng Ye, Bo Zhang, Hancheng Ye, Baopu Li, Yancheng Cai, and Tao Chen. 2023a. Rethinking of Feature Interaction for Multi-task Learning on Dense Prediction. *arXiv preprint arXiv:2312.13514* (2023).
- Jingdong Zhang, Jiayuan Fan, Peng Ye, Bo Zhang, Hancheng Ye, Baopu Li, Yancheng Cai, and Tao Chen. 2025b. BridgeNet: Comprehensive and Effective Feature Interactions via Bridge Feature for Multi-Task Dense Predictions. *IEEE Transactions on Pattern Analysis and Machine Intelligence* (2025).
- Jiaming Zhang, Kailun Yang, Hao Shi, Simon Reiß, Kunyu Peng, Chaoxiang Ma, Haodong Fu, Philip HS Torr, Kaiwei Wang, and Rainer Stiefelhagen. 2024. Behind every domain there is a shift: Adapting distortion-aware vision transformers for panoramic semantic segmentation. *IEEE Transactions on Pattern Analysis and Machine Intelligence* 46, 12 (2024), 8549–8567.
- Jingdong Zhang, Hanrong Ye, Xin Li, Wenping Wang, and Dan Xu. 2025c. Multi-task label discovery via hierarchical task tokens for partially annotated dense predictions. In *Proceedings of the 33rd ACM International Conference on Multimedia*. 719–728.
- Jingdong Zhang, Lingzhi Zhang, Qing Liu, Mang Tik Chiu, Connelly Barnes, Yizhou Wang, Haoran You, Xiaoyang Liu, Yuqian Zhou, Zhe Lin, et al. 2025d. UNISER: A Foundation Model for Unified Soft Effects Removal. *arXiv preprint arXiv:2511.14183* (2025).
- Lvmin Zhang, Anyi Rao, and Maneesh Agrawala. 2023b. Adding conditional control to text-to-image diffusion models. In *Proceedings of the IEEE/CVF international conference on computer vision*. 3836–3847.
- Zhenyu Zhang, Zhen Cui, Chunyan Xu, Zequn Jie, Xiang Li, and Jian Yang. 2018. Joint task-recursive learning for semantic segmentation and depth estimation. In *ECCV*. 235–251.
- Zhenyu Zhang, Zhen Cui, Chunyan Xu, Yan Yan, Nicu Sebe, and Jian Yang. 2019. Pattern-affinitive propagation across depth, surface normal and semantic segmentation. In *CVPR*. 4106–4115.
- Junwei Zheng, Ruiping Liu, Yufan Chen, Kunyu Peng, Chengzhi Wu, Kailun Yang, Jiaming Zhang, and Rainer Stiefelhagen. 2024. Open panoramic segmentation. In *European Conference on Computer Vision*. Springer, 164–182.
- Jia Zheng, Junfei Zhang, Jing Li, Rui Tang, Shenghua Gao, and Zihan Zhou. 2020. Structured3d: A large photo-realistic dataset for structured 3d modeling. In *European Conference on Computer Vision*. Springer, 519–535.
- Bolei Zhou, Hang Zhao, Xavier Puig, Tete Xiao, Sanja Fidler, Adela Barriuso, and Antonio Torralba. 2019. Semantic understanding of scenes through the ade20k dataset. *International Journal of Computer Vision* 127, 3 (2019), 302–321.



Fig. 10. More results on in-the-wild data samples.